Inorganic Chemistry

Article

pubs.acs.org/IC

The Flexible $Ba_7UM_2S_{12.5}O_{0.5}$ (M = V, Fe) Compounds: Syntheses, Structures and Spectroscopic, Resistivity, and Electronic Properties

Adel Mesbah,[†] Wojciech Stojko,[†] Christos D. Malliakas,[†] Sébastien Lebègue,[‡] Nicolas Clavier,[§] and James A. Ibers*,[†]

[†]Department of Chemistry, Northwestern University, 2145 Sheridan Road, Evanston, Illinois 60208-3113, United States

[‡]Laboratoire de Cristallographie, Résonance Magnétique, et Modélisations CRM2 (UMR UHP-CNRS 7036), Faculté des Sciences et Techniques, Université de Lorraine, BP 70239, Boulevard des Aiguillettes, 54506 Vandoeuvre-lès-Nancy Cedex, France

[§]ICSM-UMR 5257 CNRS/CEA/UM2/ENSCM, Site de Mercoule bat 426, BP 17171, 30207 Bagnols/Ceze, France

Supporting Information

ABSTRACT: Two new compounds, $Ba_7UV_2S_{12.5}O_{0.5}$ and $Ba_7UFe_2S_{12.5}O_{0.5}$, have been synthesized in fused-silica tubes by the direct combinations of V or Fe with U, BaS, and S at 1223 K. The compound $Ba_7UV_2S_{12.5}O_{0.5}$ crystallizes at 100 K in the $Cs_7Cd_3Br_{17}$ structure type in space group D_{4h}^{18}–*I4/mcm* of the tetragonal system. The compound $Ba_7UFe_2S_{12.5}O_{0.5}$ crystallizes at 100 K in space group D_{4h}^{5}–*P4/mbm* of the tetragonal system. The structures are very similar with V/S or Fe/S networks in which Ba atoms reside as well as channels large enough to accommodate additional Ba atoms and infinite linear US_5O chains. Each U atom is octahedrally coordinated to four equatorial S atoms, one axial S atom, and one axial O atom. The Fe/S network contains a S−S single bond, whereas the V/S network does not. The result is that the Fe^{3+} compound charge balances with 7 Ba^{2+}, U^{4+}, 2 Fe^{3+}, 10.5 S^{2-}, S_2^{2-}, and 0.5 O^{2-}, whereas the V^{4+} compound charge balances with 7 Ba^{2+}, U^{4+}, 2 V^{4+}, 12.5 S^{2-}, and 0.5 O^{2-}. Other differences between these two compounds have been characterized by Raman spectroscopy and resistivity measurements. DFT calculations have provided insight into the nature of their bonding. The overall structural motif of $Ba_7UV_2S_{12.5}O_{0.5}$ and $Ba_7UFe_2S_{12.5}O_{0.5}$ offers a remarkable flexibility in terms of the oxidation state of the incorporated transition metal.

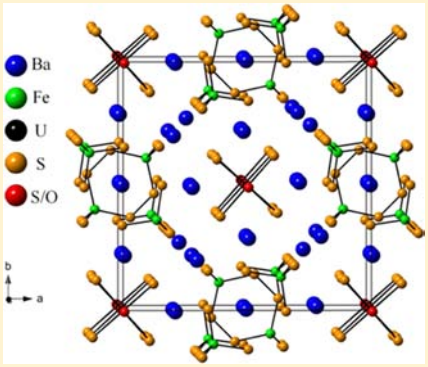

INTRODUCTION

There is considerable activity directed toward the discovery of new materials comprising actinides and transition metals because of the potential interplay between the localized 5f electrons of the actinides and the conduction electrons of the d metals.[1−7] Such materials show a variety of exciting physical properties, such as superconductivity and magnetism. In the family of actinide (An) chalcogenides (Q = S, Se, or Te), many solid-state compounds have been synthesized.[8−11] In particular, those containing 3d metals (M) have shown differing magnetic, electrical, or optical properties. Included among the ternaries are MU_8Q_{17},[12−18] $MAnQ_3$,[10,12,19−23] and $Cu_2U_3Q_7$.[24] Quaternaries with an alkali metal (A) or Tl include $ACuAnQ_3$,[9,11,25] $A_6Cu_{12}U_2S_{15}$,[26] $Tl_3Cu_4USe_6$,[27] $KCuThS_3$, $K_2Cu_2ThS_4$, $K_3Cu_3Th_2S_7$,[28] $K_2Cu_3US_5$,[29] and $CsTiUTe_5$.[30] Recently, we have extended the study of actinide chalcogenides to include alkaline-earth elements(Ak) through the syntheses and characterization of a number of Ba/An/Q compounds: $BaUS_3$,[31−33] $AkAn_2Q_5$,[31,34] $Ba_{3.69}US_6$,[31] Ba_2AnS_6,[35] $Ba_2Cu_2AnS_5$,[36,37] $Ba_4Cr_2US_9$,[38] and $Ba_8Hg_3U_3S_{18}$.[39]

In an attempt to extend the known Ba-containing actinide chalcogenides to include 3d elements other than Cu or Cr, the unexpected quintary compounds $Ba_7UV_2S_{12.5}O_{0.5}$ and $Ba_7UFe_2S_{12.5}O_{0.5}$ were synthesized, their O contents arising from the fused-silica tubes in which the reactions were carried out. The structures of these compounds, though similar, differ in an important way. The remarkably flexible structural motif accommodates a V^{4+} atom in $Ba_7UV_2S_{12.5}O_{0.5}$ to be contrasted with $Ba_7UFe_2S_{12.5}O_{0.5}$ in which a S−S single bond is formed and the Fe^{3+} atom is found. We describe these results here along with Raman spectra, resistivity measurements, and DFT calculations.

EXPERIMENTAL METHODS

Syntheses. The following reactants were used as obtained: Fe (Alfa Aesar, 99.9%), V (Alfa Aesar, 99.5%), BaS (Alfa Aesar, 99.7%), and S (Mallinckrodt, 99.6%). ^{238}U powder was obtained by hydridization and decomposition of U turnings (ORNL) in a modification[40] of a literature method.[41] All reactions were performed in carbon-coated fused-silica tubes. The starting mixtures were loaded into such tubes under an Ar atmosphere in a glovebox. Then, the tubes were evacuated to 10^{-4} Torr, flame-sealed, and placed in a computer-controlled furnace. Each reaction mixture was heated to 1223 K in 48 h, kept at 1223 K for 8 days, and then cooled to 473 K at a rate of 2 K h^{-1} when the furnace was turned off. Elemental composition was determined semiquantitatively with an EDX-equipped Hitachi S-3400 SEM. However, the oxygen content could not be quantified.

Received: July 19, 2013
Published: October 9, 2013

   dx.doi.org/10.1021/ic401871x | *Inorg. Chem.* 2013, 52, 12057−12063

Table 1. Crystal Data and Structure Refinements for $Ba_7UV_2S_{12.5}O_{0.5}$ and $Ba_7UFe_2S_{12.5}O_{0.5}$[a]

	$Ba_7UV_2S_{12.5}O_{0.5}$	$Ba_7UFe_2S_{12.5}O_{0.5}$	$Ba_7UFe_2S_{12.5}O_{0.5}$
fw (g mol^{-1})	1710.04	1719.86	1719.86
temperature (K)	100	100	360
space group	D_{4h}^{18}–$I4/mcm$	D_{4h}^{5}–$P4/mbm$	D_{4h}^{5}–$P4/mbm$
a (Å)	16.0749(8)	15.8750(4)	15.9437(3)
c (Å)	9.5003(5)	9.6296(2)	9.6535(2)
V (Å^3)	2454.9(3)	2426.8(1)	2453.9(1)
ρ (g cm^{-3})	4.627	4.707	4.655
μ (mm^{-1})	19.376	20.026	19.804
$R(F)^b$	0.0214	0.0139	0.0209
$R_w(F_o^2)^c$	0.0527	0.0322	0.0446

[a] $Z = 4$, $\lambda = 0.71073$ Å. [b] $R(F) = \sum||F_o| - |F_c||/\sum|F_o|$ for $F_o^2 > 2\sigma(F_o^2)$. [c] $R_w(F_o^2) = \{\sum w(F_o^2 - F_c^2)^2]/\sum wF_o^4\}^{1/2}$. For $F_o^2 < 0$, $w^{-1} = \sigma^2(F_o^2)$; for $F_o^2 \geq 0$, $w^{-1} = \sigma^2(F_o^2) + (qF_o^2)^2$, where $q = 0.0178$ for $Ba_7UV_2S_{12.5}O_{0.5}$, 0.0086 for $Ba_7UFe_2S_{12.5}O_{0.5}$ at (100 K) and 0.0163 (360 K).

Synthesis of $Ba_7UV_2S_{12.5}O_{0.5}$. Black blocks were obtained by the reaction of BaS (42.7 mg, 0.25 mmol), V (4.3 mg, 0.084 mmol), U (20 mg, 0.084 mmol), and S (8 mg, 0.25 mmol). The black blocks isolated in approximately 50 wt % yield (based on Ba) showed the presence of Ba:V:U:S in the approximate atomic ratio 7:2:1:13. Other platelike black crystals showed the composition U:S = 1:1, attributable to UOS.

Synthesis of $Ba_7UFe_2S_{12.5}O_{0.5}$. Black blocks were isolated from the stoichiometric reaction of BaS (99 mg, 0.58 mmol), Fe (9.47 mg, 0.168 mmol), U (20 mg, 0.084 mmol), and S (16 mg, 0.5 mmol). The yield was about 90 wt %. Analysis showed Ba:Fe:U:S in the approximate atomic ratio 7:2:1:13.

Structure Determinations. Single-crystal X-ray diffraction data for $Ba_7UV_2S_{12.5}O_{0.5}$ and $Ba_7UFe_2S_{12.5}O_{0.5}$ were collected with the use of graphite-monochromatized Mo Kα radiation ($\lambda = 0.71073$ Å) at 100 K on a Bruker APEX2 diffractometer.[42] Data were also collected at 360 K from a single crystal of $Ba_7UFe_2S_{12.5}O_{0.5}$. The data collection strategy was optimized with the algorithm COSMO in the program APEX2[42] as a series of 0.3 scans in ω and φ. The exposure time was 10 s/frame. The crystal-to-detector distance was 6 cm. The collection of data, cell refinement, and data reduction were carried out with the use of the program APEX2.[42] Face-indexed absorption, incident beam, and decay corrections were performed with the use of the program SADABS.[43] Both structures were solved and refined with the use of the SHELX13 programs.[44] The program STRUCTURE TIDY[45] in PLATON[46] was used to standardize the atomic positions. Further details are given in Table 1 and in the Supporting Information.

Although the EDX results did not quantify the ≈0.5 wt % O, it became evident in the refinements of each of the V and Fe structures that the compounds are quintaries and contain oxygen. The evidence consisted of improved agreement indices, and the fact that the U atoms are disordered along the c axis in such a way as to enable each to have a normal U–S distance as well as a normal U–O distance. Further details are provided below.

μ-Raman Spectroscopy. Raman spectra were recorded with a Horiba-Jobin Yvon Aramis apparatus equipped with an edge filter and a Nd:YAG laser (532 nm) that delivered 60 mW at the sample surface. To avoid any laser-induced degradation of the surface, the power was reduced to about 15 mW by the means of optical filters. The laser beam was then focused on a sample using an Olympus BX 41 microscope, resulting in a spot area of about 1 μm^2. For each spectrum, a dwell time of 30–60 s was used with an average of four scans. Data were collected on five different single crystals.

Resistivity Measurements. Two-probe temperature-dependent resistivity data were collected using a homemade resistivity apparatus equipped with a Keithley 617 electrometer and a high-temperature vacuum chamber controlled by a K-20 MMR system. Data acquisition was controlled by custom-written software. Initially, electrical contacts were made with fast drying silver paint (Ted Pella, Inc.; Electrodag 1415M), but silver was found to react with $Ba_7UFe_2S_{12.5}O_{0.5}$ at high temperature. Therefore, PELCO isopropanol-based graphite paint was used to attach Cu wires of 0.025 mm in thickness (Omega) to the samples. The direct current was applied along an arbitrary direction. Measurements were done on single crystals with the dimensions of 0.320 × 0.340 × 0.150 mm for $Ba_7UV_2S_{12.5}O_{0.5}$ and 0.210 × 0.250 × 0.100 mm for $Ba_7UFe_2S_{12.5}O_{0.5}$.

Ab Initio Calculations. Calculations were performed using density functional theory[47] (DFT) with the generalized gradient approximation[48] (GGA) for the exchange correlation potential, as implemented in the Vienna Ab initio Simulation Package (VASP).[49,50] The wave function was expanded following the projector augmented wave method[51] using the default cutoff for the plane-wave part. The cell and atom positions were converted from the experimental values using the cif2cell program.[52] The averaged position was taken for disordered U atoms. To integrate over the Brillouin zone, a mesh of 1 × 1 × 2 was used for the two compounds. Spin polarization was allowed, and the various possible magnetic configurations in the crystallographic cell were compared in terms of total energy in order to identify the ground-state magnetic arrangement. Then, the reconstructed charge density[53] in real space was generated from the converged DFT calculation in order to perform Bader's analysis.[54,55]

RESULTS

Syntheses. The compounds $Ba_7UV_2S_{12.5}O_{0.5}$ and $Ba_7UFe_2S_{12.5}O_{0.5}$ were synthesized at 1223 K by direct combination of V or Fe with U, BaS, and S, respectively. The yield of small black blocks of $Ba_7UV_2S_{12.5}O_{0.5}$ was about 50 wt %. The rest of the product was found to be UOS. Black blocks of $Ba_7UFe_2S_{12.5}O_{0.5}$ were obtained in a high yield of about 90 wt %. The presence of UOS was again detected. UOS is a highly stable byproduct of syntheses of actinide chalcogenides.[35,56] In the present syntheses, the unexpected O content in the compounds of interest arose from the etching of the silica tubes.

Structure of $Ba_7UV_2S_{12.5}O_{0.5}$. The compound $Ba_7UV_2S_{12.5}O_{0.5}$ crystallizes in the $Cs_7Cd_3Br_{13}$ structure type[57,58] with four formula units in space group D_{4h}^{18}–$I4/mcm$ of the tetragonal system in a cell of dimensions $a = 16.0749(8)$ Å and $c = 9.5003(5)$ Å at 100 K. The asymmetric unit contains one disordered U1 atom (site symmetry 4.., Wyckoff position 8f), one V1 atom (m.2m, 8h), three Ba atoms Ba1, Ba2, Ba3 (.2., 16j; m.2m, 8h; $\bar{4}$2m, 4b, respectively), three S atoms S1, S2, S3 (..m, 16l; m.., 16k; and m.., 16k, respectively), and an O1/S4 mixed site (422, 4a). The asymmetric unit of $Cs_7Cd_3Br_{13}$ contains three Cs, two Cd, and 4 Br positions. The correspondence between the structures of $Ba_7UV_2S_{12.5}O_{0.5}$ and $Cs_7Cd_3Br_{13}$ is Ba with Cs, V with Cd, S with Br, O with Br, and the "average" U with Cd. In essence, VS_4 tetrahedra replace $CdBr_4$ tetrahedra and US_5O octahedra replace $CdBr_6$ octahedra.

A general view down the c axis of the structure of $Ba_7UV_2S_{12.5}O_{0.5}$ is presented in Figure 1a. The structure

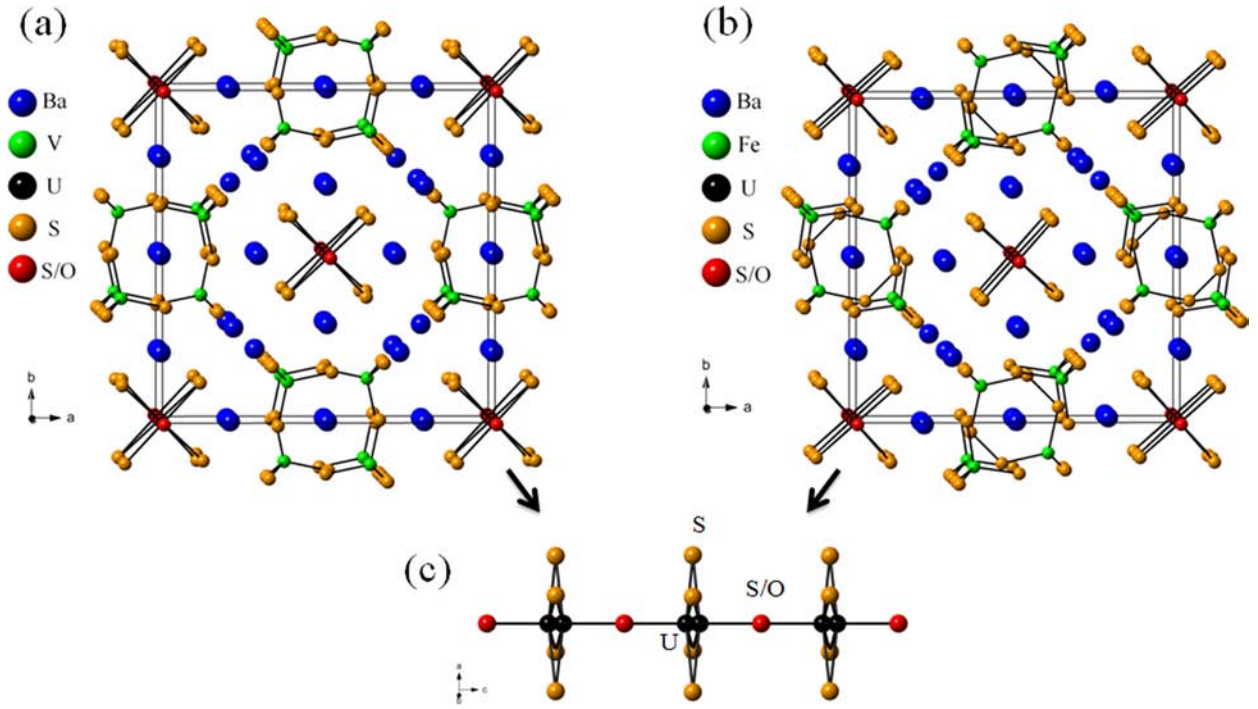

Figure 1. Crystal structures of the (a) $Ba_7UV_2S_{12.5}O_{0.5}$ and (b) $Ba_7UFe_2S_{12.5}O_{0.5}$ viewed down the *c* axis. (c) The US_5O chain in both compounds.

consists of a V/S network in which Ba atoms reside, as well as channels large enough to accommodate additional Ba atoms that surround infinite linear US_5O chains (Figure 1c). Each U1 atom is octahedrally coordinated to four S3 atoms, one S4 atom, and one O atom. The only chemical reasonable interpretation of these chains is shown in Figure 2. The U1

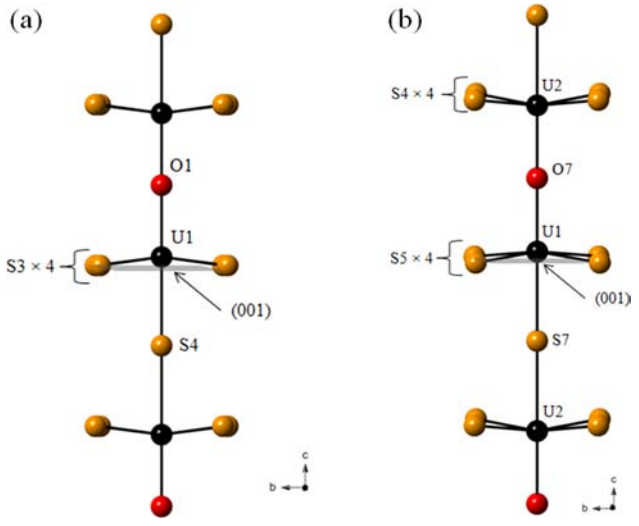

Figure 2. Infinite linear chains in the structure of (a) $Ba_7UV_2S_{12.5}O_{0.5}$ and (b) $Ba_7UFe_2S_{12.5}O_{0.5}$ formed by the connection of the US_5O octahedra along the *c* axis.

atom can sit either above or below the (001) plane at 0,0,*z* or 0,0,−*z*, but not at both sites because this leads to a U−U distance of 0.503 Å. If the U1 atom is above the plane, then it is connected to atom O1 further up the *c* axis (U1−O1 = 2.1236(5) Å) and to atom S4 on the *c* axis below the plane (U1−S4 = 2.6265(5) Å). If the U1 atom is below the plane, then the O1 atom is also below the plane and the S4 atom is above the plane. By symmetry, the up/down U atoms alternate and hence so do the O1/S4 atoms (Figure 2). The four S3 atoms form a plane that is strictly perpendicular to the *c* axis at *z* = 0 (U1−S3 = 2.679(1) Å); hence the S3 atom is not disordered. The U1−S distances of 2.679(1) and 2.6265(5) Å are typical for octahedrally coordinated U^{4+} and may be compared, for example, with those in $BaUS_3$[31] of 2.668(1)−2.696(1)Å, $Ba_2Cu_2US_5$[36] of 2.673(2)−2.770(1)Å, and Li_2US_3[59] of 2.603−2.677 Å. The U1−O distance of 2.1236(5) Å is typical, for example, 2.166 Å in V_2UO_6[60] and 2.136 Å in UP_4O_{12}.[61]

Each V atom is surrounded by two S1 and two S2 atoms to form a tetrahedron (Figure 3a), with the V−S distances of 2 × 2.180(1) and 2 × 2.195(1) Å. These distances may be compared with those of 2.190 Å found for tetrahedrally coordinated V^{4+} in $As_3Cu_{13}VS_{16}$.[62]

Each Ba atom is coordinated by eight S atoms. Ba1 atom is coordinated to four S1 atoms, two S3 atoms, and two S2 atoms with Ba1−S distances between 3.2719(9) and 3.4310(9) Å. The Ba2 atom is also coordinated to four S1 atoms, two S3 atoms, and two S2 atoms with Ba2−S distances between 3.012(1) and 3.422(1) Å. Finally, each Ba3 atoms is coordinated by eight S2 atoms at a distance of 3.417(1) Å. The Ba atoms lie in these channels. These distances are typical for barium chalcogenides, for example, $BaUS_3$, Ba_2US_6, $Ba_{3.69}US_6$, and BaU_2S_5.[31]

Structure of $Ba_7UFe_2S_{12.5}O_{0.5}$. The compound $Ba_7UFe_2S_{12.5}O_{0.5}$ crystallizes in a new structure type with four formula units in the tetragonal space group D_{4h}^5−*P*4/*mbm* with *a* = 15.8750(4) Å and *c* = 9.6296(2) Å at 100 K. The asymmetric units contains two U atoms (site symmetry 4..; Wyckoff positions 4e, 4e), two Fe atoms (m.2m; 4h, 4g), four Ba atoms Ba1, Ba2, Ba3, B4 (1, m.2m, m.2m, 2.mm; 16l, 4h, 4g, 4f), and six S atoms, S1, S2(..m; 8k, 8k) and S3−S6 (all m..; 8j, 8j, 8i, 8i), and the seventh mixed position S7/O7 (4..; 4e).

dx.doi.org/10.1021/ic401871x | *Inorg. Chem.* 2013, 52, 12057−12063

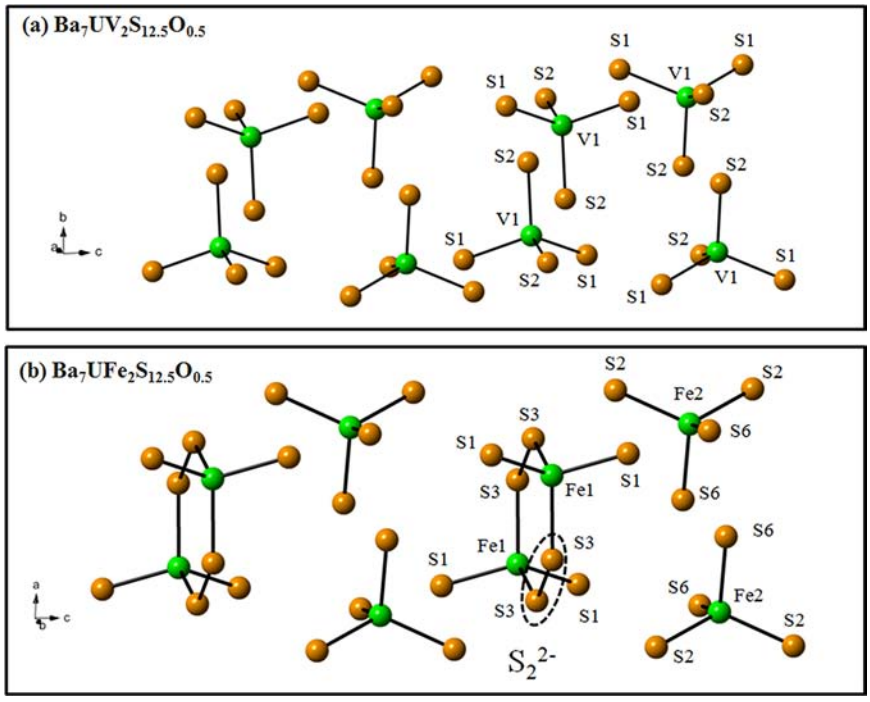

Figure 3. Arrangements of VS_4 tetrahedra in (a) $Ba_7UV_2S_{12.5}O_{0.5}$ and the FeS_4 tetrahedra and Fe_2S_8 rings in (b) $Ba_7UFe_2S_{12.5}O_{0.5}$.

Table 2. Selected Interatomic Distances (Å) and Angles (deg) for $Ba_7UV_2S_{12.5}O_{0.5}$ and $Ba_7UFe_2S_{12.5}O_{0.5}$

	$Ba_7UV_2S_{12.5}O_{0.5}$		$Ba_7UFe_2S_{12.5}O_{0.5}$	
T (K)	100		100	360
U1−S3 × 4	2.679(1)	U1−S5 × 4	2.5959(8)	2.599(1)
U1−S4	2.6265(5)	U1−S7	2.667(2)	2.682(2)
U1−O1	2.1236 (5)	U1−O7	2.155(2)	2.160(2)
V1−S1 × 2	2.180(1)	U2−S4 × 4	2.5982(8)	2.603(1)
V1−S2 × 2	2.195(1)	U2−S7	2.640(2)	2.643(2)
S1−V1−S1	118.97(9)	U2−O7	2.169(2)	2.169(2)
S2−V1−S1 × 4	106.15(2)	Fe1−S1 × 2	2.2287(8)	2.226(1)
S2−V1−S2	113.58(9)	Fe1−S3 × 2	2.3255(8)	2.335(1)
		Fe2−S2 × 2	2.2454(8)	2.247(1)
		Fe2−S6 × 2	2.2424(8)	2.246(1)
		S3−S3	2.153(2)	2.145(2)
		S1−Fe1−S1	120.95(5)	121.23(6)
		S1−Fe1−S3 × 4	105.37(1)	105.39(2)
		S3−Fe1−S3	114.93(5)	114.51(6)
		S6−Fe2−S6	107.19(5)	107.00(6)
		S6−Fe2−S2 × 4	107.21(1)	107.34(2)
		S2−Fe2−S2	120.20(5)	119.86(6)

A general view down the *c* axis of the structure of $Ba_7UFe_2S_{12.5}O_{0.5}$ is shown in the Figure 1b. The structure is similar to that of $Ba_7UV_2S_{12.5}O_{0.5}$, but primitive rather than body-centered. Both U positions are disordered, as are the S7/O7 positions. Each U1 atom is octahedrally coordinated to four S5 atoms (U1−S5 = 2.5959(8) Å), one S7 atom (U1−S7 = 2.667(2) Å), and one O7 atom (U1−O7 = 2.155(2) Å); each U2 atom is octahedrally coordinated to four S4 atoms (U2−S4 = 2.5982(8) Å), one S7 atom (U2−S7 = 2.640(2) Å), and one O7 atom (U2−O7 = 2.169(2) Å). These distances are typical for octahedrally coordinated U^{4+}. As in the chain in $Ba_7VU_2S_{12.5}O_{0.5}$ (Figure 2a), the infinite linear US_5O chain in $Ba_7UFe_2S_{12.5}O_{0.5}$ (Figure 2b) exhibits a similar disorder of the U and S7/O7 positions. Again, the equatorial S atoms (S4 and S5) form planes that are strictly perpendicular to the *c* axis and hence are not disordered.

The Fe atoms are tetrahedrally coordinated (Figure 3b) as are the V atoms in $Ba_7UV_2S_{12.5}O_{0.5}$. Each Fe1 atom is coordinated to two S1 and two S3 atoms (Fe1−S1 = 2.2287(8) Å, Fe1−S3 = 2.3255(8) Å); each Fe2 atom is coordinated to two S2 and two S6 atoms (Fe2−S2 = 2.2454(8) Å, Fe2−S6 = 2.2424(8) Å). However, the similarities between the structures of $Ba_7UV_2S_{12.5}O_{0.5}$ and $Ba_7UFe_2S_{12.5}O_{0.5}$ end with the bonding pattern around the Fe1 atom. The two Fe1 tetrahedra are connected together by S3−S3 pairs (with a single bond S3−S3 distance of 2.153(2) Å) to form disulfide (S_2^{2-}) bridges in a new centrosymmetric Fe_2S_8 cluster (Figure 3b). The Fe−S distances may be compared with those found for tetrahedrally coordinated Fe^{3+} in $BaFe_2S_4$[63] of 2.218(1) Å,

dx.doi.org/10.1021/ic401871x | *Inorg. Chem.* 2013, 52, 12057−12063

Na_5FeS_4[64] of 2.277(8)−2.2925(8)Å, and Na_3FeS_3[65] of 2.249−2.298 Å.

The four Ba atoms have coordination numbers of 9, 8, 8, and 10 for Ba1, Ba2, Ba3, and Ba4, respectively, with the Ba−S distances ranging between 3.0565(8) and 3.5075 (8) Å. More metrical details are given in Table 2 and in the Supporting Information.

Oxidation States. The U−S distances for both $Ba_7UV_2S_{12.5}O_{0.5}$ and $Ba_7UFe_2S_{12.5}O_{0.5}$ (Table 2) are typical for octahedrally coordinated U^{4+}. In the structure of $Ba_7UV_2S_{12.5}O_{0.5}$, there are no S−S interactions shorter than 3.5 Å. Hence, there are only S^{2-} species in the structure. Accordingly, the only way that $Ba_7UV_2S_{12.5}O_{0.5}$ can be charge-balanced is with 7 Ba^{2+}, U^{4+}, 2 V^{4+}, 12.5 S^{2-}, and 0.5 O^{2-}. In $Ba_7UFe_2S_{12.5}O_{0.5}$, there is a short interaction (S3−S3 = 2.15 Å) that corresponds to a single bond and hence to the S_2^{2-} disulfide species. All other S−S interactions are longer than 3.5 Å. Given that the Fe−S distances are essentially equal and thus involve the same oxidation state of Fe, the only way that $Ba_7UFe_2S_{12.5}O_{0.5}$ can be charge-balanced is with 7 Ba^{2+}, U^{4+}, 2 Fe^{3+}, 10.5 S^{2-}, S_2^{2-}, and 0.5 O^{2-}.

Thus, $Ba_7UV_2S_{12.5}O_{0.5}$ contains V^{4+}, whereas $Ba_7UFe_2S_{12.5}O_{0.5}$ contains Fe^{3+} rather than the unlikely Fe^{4+}. The Fe^{4+} state is avoided through the formation of Fe_2S_8 clusters in which FeS_4 tetrahedra are joined through S−S bonds. The striking nature of this unprecedented structural change is emphasized in Figure 3. This overall structural motif offers a remarkable flexibility in terms of the nature of the incorporated transition metal.

Spectroscopic Properties. The Raman spectra (Figure 4) for both compounds confirm the structural features found from the diffraction studies. First, the bands located between 300 and 400 cm^{-1} are assigned to the symmetric stretching vibrations in the FeS_4 or VS_4 tetrahedra.[66,67] Moreover, the signal is broadened significantly for $Ba_7UFe_2S_{12.5}O_{0.5}$, which we ascribe to its less symmetric structure compared with that of $Ba_7UV_2S_{12.5}O_{0.5}$. Such broadening is also evident in the region between 700 and 800 cm^{-1}, which we assign to the US_5O octahedra by comparison to the data for the UO_6 unit in the perovskite structure type.[68] The signal for $Ba_7UFe_2S_{12.5}O_{0.5}$ at 700 cm^{-1} probably corresponds to the overlap of multiple vibration bands associated with the two different U sites in the structure. The Raman spectrum of $Ba_7UFe_2S_{12.5}O_{0.5}$ also shows the characteristic vibration of the S−S bond, located at about 450 cm^{-1}. Although this vibrational mode is usually found from 480 to 520 cm^{-1} for organic compounds,[69,70] its occurrence within ring units in metal complexes can shift the band toward lower values.[71] Also, it probably overlaps with some bands related to the antisymmetric stretching modes of FeS_4,[72] which can explain the presence of a small band in this region for the $Ba_7UV_2S_{12.5}O_{0.5}$ compound. Ring deformations in the Fe_2S_8 rings in the $Ba_7UFe_2S_{12.5}O_{0.5}$ structure we assign to the intense band located at 970 cm^{-1}.

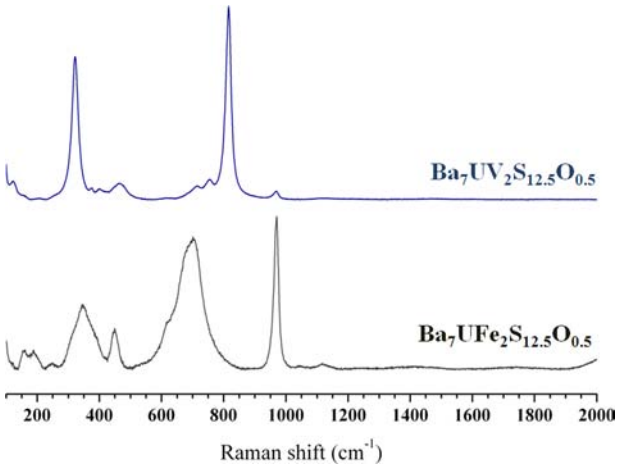

Figure 4. Raman spectra of $Ba_7UFe_2S_{12.5}O_{0.5}$ and $Ba_7UV_2S_{12.5}O_{0.5}$ in the 100−2000 cm^{-1} region.

Resistivity Behavior. Resistivity measurements (Figure 5) on single crystals of $Ba_7UV_2S_{12.5}O_{0.5}$ and $Ba_7UFe_2S_{12.5}O_{0.5}$ show semiconducting behavior. The resistivity decreases from 64500 to 6720 ohm·cm for $Ba_7UV_2S_{12.5}O_{0.5}$ and from 4780 to 610 ohm·cm for $Ba_7UFe_2S_{12.5}O_{0.5}$ as the temperature increases from 298 to 500 K. A discontinuity at around 325 K was observed for both compounds. It does not arise from phase changes, as the crystal structure of $Ba_7UFe_2S_{12.5}O_{0.5}$ determined at both 100 and 360 K does not change (Tables 1 and 2). The corresponding Arrhenius plots from the resistivity data are linear below and above the discontinuity. The activation energies below and above the 325 K discontinuity are 0.19(1) and 0.12(1) eV for $Ba_7UV_2S_{12.5}O_{0.5}$ and 0.22(1) and 0.11(1) eV for $Ba_7UFe_2S_{12.5}O_{0.5}$, respectively.

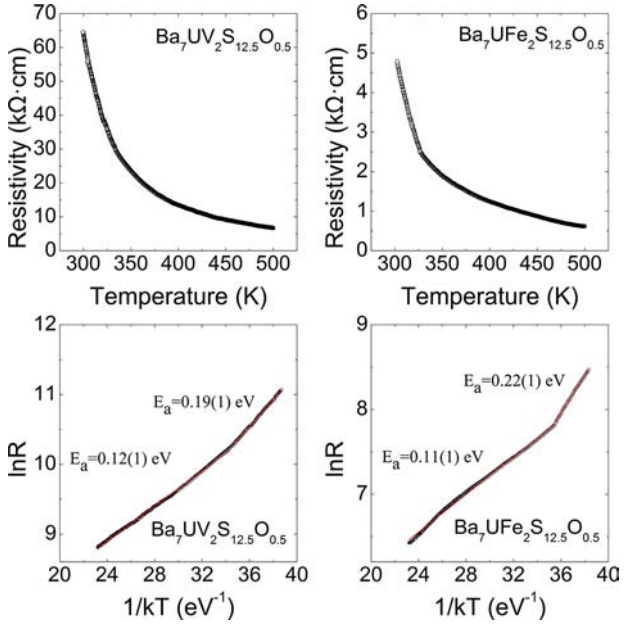

Figure 5. Resistivity and their corresponding Arrhenius plots for $Ba_7UV_2S_{12.5}O_{0.5}$ and $Ba_7UFe_2S_{12.5}O_{0.5}$.

Electronic Properties. The ground-state magnetic arrangements were obtained from a comparison of total energies. For $Ba_7UV_2S_{12.5}O_{0.5}$, the ground state is fully ferromagnetic with all U and V magnetic moments pointing in the same direction. For $Ba_7UFe_2S_{12.5}O_{0.5}$, the magnetic moments on the U atoms are arranged ferromagnetically, while the U magnetic moments are arranged antiferromagnetically among themselves.

From the calculated electron density, the number of electrons belonging to each atom in the cell was uniquely obtained from Bader's decomposition.[54,55] For $Ba_7UV_2S_{12.5}O_{0.5}$, the calculated number of electrons ranges from 7.05 to 7.2 e^- for S, 12.2 e^- for U, 8.5 e^- for Ba, 7.0 e^- for O, and 3.7 e^- for V

dx.doi.org/10.1021/ic401871x | Inorg. Chem. 2013, 52, 12057−12063

atoms. For $Ba_7UFe_2S_{12.5}O_{0.5}$, the calculated number of electrons for the S atoms ranges from 6.7 e^- (S3) to 7.2 e^- (S1−S7, except S3), U 12.2 e^-, Ba 8.5 e^-, O 7.0 e^-, and Fe 7.1 e^-. The difference in the number of electrons for the S atoms in $Ba_7UFe_2S_{12.5}O_{0.5}$ reflects the particular electronic structure of this compound, as seen by the experimental techniques. Also, these values are in agreement with our previous studies[35,37] on 5f/S systems. However, any partition scheme of the electron density gives only effective charges for each atom. Such numbers are useful to compare different systems at the same level of theory. However, sometimes they cannot be compared directly with charges derived from experiments, and caution is needed.

To have a better understanding of the electronic structure of $Ba_7UFe_2S_{12.5}O_{0.5}$, we have plotted in Figure 6 the total and

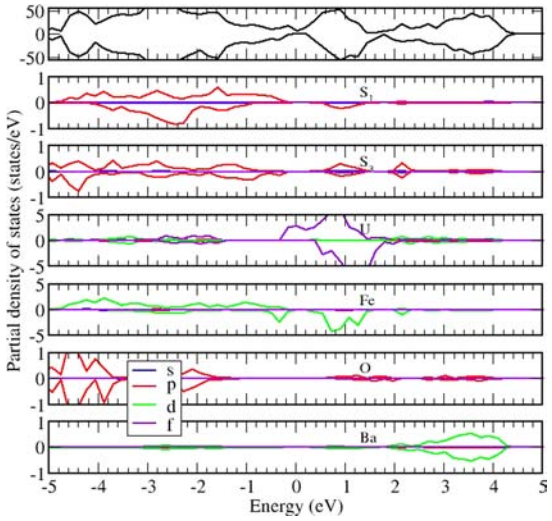

Figure 6. Total (upper plot) and partial density of states (lower plots) of $Ba_7UFe_2S_{12.5}O_{0.5}$. For each atom, the PDOS is projected onto the relevant orbitals.

partial density of states (PDOS) for each different type of atom. As seen on the total density of states (upper plot), the system has a finite spin polarization. This arises from the U and Fe atoms, as seen on the third and fourth PDOS plots. This spin polarization has a negligible effect on the Ba and O atoms (fifth and sixth PDOS plots), but its effect is clearly visible on the S atoms (first and second PDOS plots). More interestingly, the difference between the S atoms is seen from their calculated PDOS, with structures located at different energies and with different intensities. The S3 atoms are responsible for S−S bonding, as viewed in Figure 3, whereas S1 is a typical S^{2-} species, representative of the other sulfur atoms in the structure.

CONCLUSIONS

The two new actinide chalcogenides $Ba_7UV_2S_{12.5}O_{0.5}$ and $Ba_7UFe_2S_{12.5}O_{0.5}$ were synthesized at 1223 K by the direct combination of V or Fe with U, BaS, and S in fused-silica tubes. Their crystal structures are similar, although $Ba_7UV_2S_{12.5}O_{0.5}$ crystallizes in the $Cs_7Cd_3Br_{17}$ structure type, whereas $Ba_7UFe_2S_{12.5}O_{0.5}$ crystallizes in a new structure type. Both compounds feature structures with V/S or Fe/S networks in which Ba atoms reside as well as channels large enough to accommodate additional Ba atoms and infinite linear US_5O chains. Each U^{4+} species is octahedrally coordinated to four equatorial S atoms, one axial S atom, and one axial O atom. The Fe/S network contains a S−S single bond, whereas the V/S network does not. The result is that the Fe^{3+} compound charge balances with 7 Ba^{2+}, U^{4+}, 2 Fe^{3+}, 10.5 S^{2-}, S_2^{2-}, and 0.5 O^{2-}, whereas the V^{4+} compound charge balances with 7 Ba^{2+}, U^{4+}, 2 V^{4+}, 12.5 S^{2-}, and 0.5 O^{2-}. The Raman spectra of both compounds are consistent with the structural results. Both compounds are semiconductors. Their activation energies below 325 K are 0.12(1) and 1.29(1) eV for $Ba_7UV_2S_{12.5}O_{0.5}$ and $Ba_7UFe_2S_{12.5}O_{0.5}$, respectively. DFT calculations provide insight into the nature of the bonding in these compounds.

The overall structural motif of $Ba_7UV_2S_{12.5}O_{0.5}$ and $Ba_7UFe_2S_{12.5}O_{0.5}$ offers a remarkable flexibility in terms of the oxidation state of the incorporated transition metal.

ASSOCIATED CONTENT

Supporting Information

Crystallographic files in CIF format for $Ba_7UV_2S_{12.5}O_{0.5}$ and $Ba_7UFe_2S_{12.5}O_{0.5}$. This material is available free of charge via the Internet at http://pubs.acs.org.

AUTHOR INFORMATION

Corresponding Author

*E-mail: ibers@chem.northwestern.edu.

Notes

The authors declare no competing financial interest.

ACKNOWLEDGMENTS

This research was kindly supported at Northwestern University by the U.S. Department of Energy, Basic Energy Sciences, Chemical Sciences, Biosciences, and Geosciences Division and Division of Materials Science and Engineering Grant ER-15522, and by the National Science Foundation (DMR-1104965, C.D.M.). Use was made of the IMSERC X-ray Facility at Northwestern University, supported by the International Institute of Nanotechnology (IIN).

REFERENCES

(1) Sato, N. K.; Aso, N.; Miyake, K.; Shiina, R.; Thalmeier, P.; Varelogiannis, G.; Geibel, C.; Steglich, F.; Fulde, P.; Komatsubara, T. *Nature (London)* **2001**, *410*, 340−343.
(2) Baumbach, R. E.; Hamlin, J. J.; Janoschek, M.; Lum, I. K.; Maple, M. B. *J. Phys.: Condens. Matter* **2011**, *23*, 1−5.
(3) Maple, M. B. *Physica C* **2000**, *341−348*, 47−52.
(4) Griveau, J.-C.; Boulet, P.; Colineau, E.; Wastin, F.; Rebizant, J. *Physica B* **2005**, *359−361*, 1093−1095.
(5) Andreev, A. V.; Chernyavsky, A.; Izmaylov, N.; Sechovsky, V. *J. Alloys Compd.* **2003**, *353*, 12−16.
(6) Thompson, J. D.; Ekimov, E. A.; Sidorov, V. A.; Bauer, E. D.; Morales, L. A.; Wastin, F.; Sarrao, J. L. *J. Phys. Chem. Solids* **2006**, *67*, 557−561.
(7) Mougel, V.; Chatelain, L.; Pécaut, J.; Caciuffo, R.; Colineau, E.; Griveau, J.-C.; Mazzanti, M. *Nat. Chem.* **2012**, *4*, 1011−1017.
(8) Manos, E.; Kanatzidis, M. G.; Ibers, J. A. In *The Chemistry of the Actinide and Transactinide Elements*, 4th ed.; Morss, L. R., Edelstein, N. M., Fuger, J., Eds.; Springer: Dordrecht, The Netherlands, 2010; Vol. 6, pp 4005−4078.
(9) Bugaris, D. E.; Ibers, J. A. *Dalton Trans.* **2010**, *39*, 5949−5964.
(10) Narducci, A. A.; Ibers, J. A. *Chem. Mater.* **1998**, *10*, 2811−2823.
(11) Koscielski, L. A.; Ibers, J. A. *Z. Anorg. Allg. Chem.* **2012**, *638*, 2585−2593.
(12) Noël, H. *C. R. Seances Acad. Sci., Ser. C* **1974**, *279*, 513−515.
(13) Kohlmann, H.; Stöwe, K.; Beck, H. P. *Z. Anorg. Allg. Chem.* **1997**, *623*, 897−900.
(14) Noël, H. *C. R. Seances Acad. Sci., Ser. C* **1973**, *277*, 463−464.

(15) Noël, H.; Potel, M.; Padiou, J. *Acta Crystallogr., Sect. B: Struct. Crystallogr. Cryst. Chem.* **1975**, *31*, 2634−2637.
(16) Noel, H.; Troc, R. *J. Solid State Chem.* **1979**, *27*, 123−135.
(17) Oh, G. N.; Ibers, J. A. *Acta Crystallogr.* **2011**, *E67*, i46.
(18) Vovan, T.; Rodier, N. *C. R. Seances Acad. Sci., Ser. C* **1979**, *289*, 17−20.
(19) Ijjaali, I.; Mitchell, K.; Huang, F. Q.; Ibers, J. A. *J. Solid State Chem.* **2004**, *177*, 257−261.
(20) Jin, G. B.; Ringe, E.; Long, G. J.; Grandjean, F.; Sougrati, M. T.; Choi, E. S.; Wells, D. M.; Balasubramanian, M.; Ibers, J. A. *Inorg. Chem.* **2010**, *49*, 10455−10467.
(21) Narducci, A. A.; Ibers, J. A. *Inorg. Chem.* **1998**, *37*, 3798−3801.
(22) Narducci, A. A.; Ibers, J. A. *Inorg. Chem.* **2000**, *39*, 688−691.
(23) Noël, H.; Padiou, J.; Prigent, J. *C. R. Seances Acad. Sci., Ser. C* **1975**, *280*, 123−126.
(24) Daoudi, A.; Lamire, M.; Levet, J. C.; Noël, H. *J. Solid State Chem.* **1996**, *123*, 331−336.
(25) Koscielski, L. A.; Ibers, J. A. *Acta Crystallogr., Sect. E: Struct. Rep. Online* **2012**, *52*, i52−i53.
(26) Malliakas, C. D.; Yao, J.; Wells, D. M.; Jin, G. B.; Skanthakumar, S.; Choi, E. S.; Balasubramanian, M.; Soderholm, L.; Ellis, D. E.; Kanatzidis, M. G.; Ibers, J. A. *Inorg. Chem.* **2012**, *51*, 6153−6163.
(27) Bugaris, D. E.; Choi, E. S.; Copping, R.; Glans, P.-A.; Minasian, S. G.; Tyliszczak, T.; Kozimor, S. A.; Shuh, D. K.; Ibers, J. A. *Inorg. Chem.* **2011**, *50*, 6656−6666.
(28) Selby, H. D.; Chan, B. C.; Hess, R. F.; Abney, K. D.; Dorhout, P. K. *Inorg. Chem.* **2005**, *44*, 6463−6469.
(29) Gray, D. L.; Backus, L. A.; Krug von Nidda, H.-A.; Skanthakumar, S.; Loidl, A.; Soderholm, L.; Ibers, J. A. *Inorg. Chem.* **2007**, *46*, 6992−6996.
(30) Cody, J. A.; Ibers, J. A. *Inorg. Chem.* **1995**, *34*, 3165−3172.
(31) Mesbah, A.; Ibers, J. A. *J. Solid State Chem.* **2013**, *199*, 253−257.
(32) Brochu, R.; Padiou, J.; Grandjean, D. *C. R. Seances Acad. Sci., Ser. C* **1970**, *271*, 642−643.
(33) Lelieveld, R.; IJdo, D. J. W. *Acta Crystallogr., Sect. B: Struct. Crystallogr. Cryst. Chem.* **1980**, *36*, 2223−2226.
(34) Brochu, R.; Padiou, J.; Prigent, J. *C. R. Seances Acad. Sci., Ser. C* **1972**, *274*, 959−961.
(35) Mesbah, A.; Ringe, E.; Lebègue, S.; Van Duyne, R. P.; Ibers, J. A. *Inorg. Chem.* **2012**, *51*, 13390−13395.
(36) Zeng, H.-y.; Yao, J.; Ibers, J. A. *J. Solid State Chem.* **2008**, *181*, 552−555.
(37) Mesbah, A.; Lebegue., S.; Klingsporn, J. M.; Stojko, W.; Van Duyne, R. P.; Ibers, J. A. *J. Solid State Chem.* **2013**, *200*, 349−353.
(38) Yao, J.; Ibers, J. A. *Z. Anorg. Allg. Chem.* **2008**, *634*, 1645−1647.
(39) Bugaris, D. E.; Ibers, J. A. *Inorg. Chem.* **2012**, *51*, 661−666.
(40) Bugaris, D. E.; Ibers, J. A. *J. Solid State Chem.* **2008**, *181*, 3189−3193.
(41) Haneveld, A. J. K.; Jellinek, F. *J. Less-Common Met.* **1969**, *18*, 123−129.
(42) *Bruker APEX2 Version 2009.5-1 and SAINT version 7.34a Data Collection and Processing Software*; Bruker Analytical X-Ray Instruments, Inc.: Madison, WI, 2009.
(43) Sheldrick, G. M. *SADABS*; Department of Structural Chemistry, University of Göttingen: Göttingen, Germany, 2008.
(44) Sheldrick, G. M. *Acta Crystallogr., Sect. A: Found. Crystallogr.* **2008**, *64*, 112−122.
(45) Gelato, L. M.; Parthé, E. *J. Appl. Crystallogr.* **1987**, *20*, 139−143.
(46) Spek, A. L. *PLATON: A Multipurpose Crystallographic Tool*; Utrecht University: Utrecht, The Netherlands, 2008.
(47) Hohenberg, P.; Kohn, W. *Phys. Rev.* **1964**, *136*, 864−871.
(48) Perdew, J. P.; Burke, K.; Ernzerhof, M. *Phys. Rev. Lett.* **1996**, *77*, 3865−3868.
(49) Kresse, G.; Forthmüller, J. *Comput. Mater. Sci.* **1996**, *6*, 15−50.
(50) Kresse, G.; Joubert, D. *Phys. Rev. B* **1999**, *59*, 1758−1775.
(51) Blöchl, P. E. *Phys. Rev. B* **1994**, *50*, 17953−17979.
(52) Björkman, T. *Comput. Phys. Commun.* **2011**, *182*, 1183−1186.
(53) Aubert, E.; Lebègue, S.; Marsman, M.; Thu Bui, T. T.; Jelsch, C.; Dahaoui, S.; Espinosa, E.; Angyán, J. G. *J. Phys. Chem.* **2011**, *A115*, 14484−14494.
(54) Bader, R. F. W. *Atoms in Molecules: A Quantum Theory*; International Series of Monographs on Chemistry; Oxford University Press, Inc.: New York, 1990; Vol. *22*.
(55) Tang, W.; Sanville, E.; Henkelman, G. *J. Phys.: Condens. Matter* **2009**, *21*, 084204.
(56) Koscielski, L. A.; Ringe, E.; Van Duyne, R. P.; Ellis, D. E.; Ibers, J. A. *Inorg. Chem.* **2012**, *51*, 8112−8118.
(57) Marsh, R. E. *J. Solid State Chem.* **1993**, *105*, 607−608.
(58) Sieber, K. D.; Bryan, P. S.; Luss, H. R.; Hobson, J. L.; Sever, B. R.; Trauernicht, D. P.; Ferranti, S. A.; Todd, L. B. *J. Solid State Chem.* **1992**, *100*, 1−8.
(59) Masuda, H.; Fujino, T.; Sato, N.; Yamada, K.; Wakeshima, M. *J. Alloys Compd.* **1999**, *284*, 117−123.
(60) Kovba, L. M. *Radiokhimiya* **1971**, *13*, 909−910.
(61) Linde, S. A.; Gorbunova, Y. E.; Lavrov, A. V. *Zh. Neorg. Khim.* **1983**, *28*, 1391−1395.
(62) Orlandi, P.; Merlino, S.; Duchi, G.; Vezzalini, G. *Can. Mineral.* **1981**, *19*, 423−427.
(63) Swinnea, J. S.; Steinfink, H. *J. Solid State Chem.* **1980**, *32*, 329−334.
(64) Klepp, K. O.; Bronger, W. *Z. Anorg. Allg. Chem.* **1986**, *532*, 23−30.
(65) Mueller, P.; Bronger, W. *Z. Naturforsch., B: Anorg. Chem., Org. Chem.* **1979**, *34*, 1264−1266.
(66) Yachandra, V. K.; Hare, J.; Moura, I.; Spiro, T. G. *J. Am. Chem. Soc.* **1983**, *105*, 6455−6461.
(67) Czernuszewicz, R. S.; LeGall, J.; Moura, I.; Spiro, T. G. *Inorg. Chem.* **1986**, *25*, 696−700.
(68) Moreira, A. F. L.; García-Flores, A. F.; Granado, E.; Massa, N. E.; Pinacca, R. M.; Pedregosa, J. C.; Carbonio, R. E.; Muñoz, A.; Martínez-Lope; Alonso, J. A.; del Campo, L.; De Sousa Meneses, D.; Echegut, P. *Vib. Spectrosc.* **2010**, *54*, 142−147.
(69) Bastian, E. J., Jr.; Martin, R. B. *J. Phys. Chem.* **1973**, *77*, 1129−1133.
(70) Van Wart, H. E.; Lewis, A.; Scheraga, H. A.; Saeva, F. D. *Proc. Natl. Acad. Sci. U.S.A.* **1973**, *70*, 2619−2623.
(71) Young, D. M.; Schimek, G. L.; Kolis, J. W. *Inorg. Chem.* **1996**, *35*, 7620−7625.
(72) Babo, J.-M.; Jouffret, L.; Lin, J.; Villa, E. M.; Albrecht-Schmitt, T. E. *Inorg. Chem.* **2013**, *52*, 7747−7751.